Mobility Tracking in Cellular Networks Using Particle Filtering

L. Mihaylova, *Member, IEEE*, D. Angelova, S. Honary, D. R. Bull, *Senior Member, IEEE*, C. N. Canagarajah, *Member, IEEE*, and B. Ristic, *Member, IEEE*

***Abstract*— Mobility tracking based on data from wireless cellular networks is a key challenge that has been recently investigated both from a theoretical and practical point of view. This paper proposes Monte Carlo techniques for mobility tracking in wireless communication networks by means of received signal strength indications. These techniques allow for accurate estimation of Mobile Station's (MS) position and speed. The command process of the MS is represented by a first-order Markov model which can take values from a finite set of acceleration levels. The wide range of acceleration changes is covered by a set of preliminary determined acceleration values. A particle filter and a Rao-Blackwellised particle filter are proposed and their performance is evaluated both over synthetic and real data. A comparison with an Extended Kalman Filter (EKF) is performed with respect to accuracy and computational complexity. With a small number of particles the RBPF gives more accurate results than the PF and the EKF. A posterior Cramér Rao lower bound (PCRLB) is calculated and it is compared with the filters' root-mean-square error performance.**

***Index Terms*— Mobility tracking, wireless networks, hybrid systems, sequential Monte Carlo methods, Rao-Blackwellisation.**

I. Introduction

MOBILITY tracking is one of the most important features of wireless cellular communication networks [1]. Data from two types of station are usually used: *base stations* (BSs) the position of which is known, and *mobile stations* (MSs) or mobile users for which location and motion are estimated.

Mobility tracking techniques can be divided in two groups [2]: *i*) methods in which the position, speed and possibly the acceleration are estimated, and *ii*) conventional geo-location techniques, which only estimate the position coordinates. Previous approaches for mobility tracking rely on Kalman filtering [2]–[4], hidden semi-Markov models [4]–[6] and sequential Monte Carlo (MC) filtering [7].

Manuscript received November 17, 2005; revised October 23, 2006 and April 16, 2007; accepted July 3, 2007. The associate editor coordinating the review of this paper and approving it for publication was F. Daneshgaran.

L. Mihaylova is with Lancaster University, Dept. of Communication Systems, UK (email: mila.mihaylova@lancaster.ac.uk).

D. Angelova is with the Bulgarian Academy of Sciences, Bulgaria (email: donka@bas.bg).

S. Honary is with HW Communications Ltd., UK (email: Souroush@hwcomms.com).

D. Bull and N. Canagarajah are with the Dept. of Electrical and Electronic Engineering, Univ. of Bristol, UK (email: {dave.bull, nishan.canagarajah}@bristol.ac.uk).

B. Ristic is with DSTO, Australia (email: branko.ristic@dsto.defence.gov.au).

Digital Object Identifier 10.1109/TWC.2007.05912.

Two types of measurements are usually used: pilot signal strength from different BSs measured at the mobile unit and the corresponding propagation times.

The Kalman-filtering algorithms developed in [2] for real-time tracking of a MS in cellular networks have limitations due to the necessity for linearisation. This leads to the shortcomings in accuracy caused by this approximation. The two algorithms proposed in [2] use the pilot signal strengths from neighbouring BSs (i.e., the *Received Signal Strength Indication (RSSI)*), although signal measurements such as time-of-arrival (TOA) are also suitable. The model of the MS is considered to be linear, driven by a discrete command process corresponding to the MS acceleration. The command process is modelled as a semi-Markov process over a finite set of acceleration levels. The first algorithm in [2] consists of an averaging filter for processing pilot signal strength measurements and two Kalman filters, one to estimate the discrete command process and the other to estimate the mobility state. The second algorithm employs a single Kalman filter without pre-filtering the measurements and is able to track a MS even when a limited set of pilot signal measurements is available. Both proposed algorithms can be used to predict future mobility behaviour, which can be utilised in resource allocation applications.

Yang and Wang [7] developed an MC algorithm for joint mobility tracking and hard handoff detection in cellular networks. In their work, mobility tracking involves on-line estimation of the location and speed of the mobile, whereas *handoff detection* involves on-line prediction of the pilot signal strength at some future time instants. The optimal solution of both problems is prohibitively complex due to the nonlinear nature of the system. The MC joint mobility tracking and handoff detection algorithm designed in [7] is compared with a modified EKF and it is shown that the MC technique provides much better accuracy than the EKF.

In this paper we focus on mobility tracking based on signal strength measurements. In contrast to previous work [2], [3], [7], [8], mobility tracking is formulated as an estimation problem of *hybrid systems* which have a base state vector and a mode (modal) state vector. The base states are continuously evolving, whilst the modal states can undergo abrupt changes. This formulation together with the sequential MC approach provides us with a powerful tool for mobility tracking. A particle filter (PF) and a Rao-Blackwellised particle filter (RBPF) are developed and their performance investigated compared to an EKF with respect to accuracy and computational complexity.

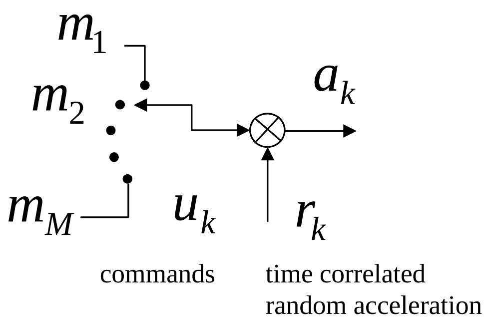

Fig. 1. Structure of the mobility acceleration chain.

The structure of the paper is as follows. Section II formulates the problem. Section III presents the mobility state and observation models. A particle filter for mobility estimation in wireless cellular networks is presented in Section IV and a Rao-Blackwellised particle filter is designed in Section V. Section VI considers the relevant PCRLB. The performance of the designed algorithms is evaluated using synthetic and real data in Section VII. Finally, conclusions and ongoing research issues are highlighted in Section VIII.

II. Problem formulation

We consider the problem of mobility tracking in cellular networks within the sequential MC framework. The dynamics of the mobility unit is described by the equation

$$\boldsymbol{x}_k = \boldsymbol{f}(\boldsymbol{x}_{k-1}, \boldsymbol{m}_k, \boldsymbol{u}_k, \boldsymbol{w}_k), \tag{1}$$

where $\boldsymbol{x}_k \in \mathbb{R}^{n_x}$ is the system *base* state, $\boldsymbol{u}_k \in \mathbb{R}^{n_u}$ specifies the command process, and $\boldsymbol{w}_k \in \mathbb{R}^{n_w}$ is the state noise, with $k \in \mathbb{N}$ being the discrete time and $\mathbb{N}$ is the set of natural numbers. The *modal (discrete) state* $\boldsymbol{m}_k$ characterising the different system modes (regimes), can take values over a finite set $\mathbb{M}$, i.e., $\boldsymbol{m}_k \in \mathbb{M}$.

The measurement equation is of the form

$$\boldsymbol{z}_k = \boldsymbol{h}(\boldsymbol{x}_k, \boldsymbol{v}_k), \tag{2}$$

where $\boldsymbol{z}_k \in \mathbb{R}^{n_z}$ is the observation, and $\boldsymbol{v}_k \in \mathbb{R}^{n_v}$ is the measurement noise. Functions $\boldsymbol{f}(.)$ and $\boldsymbol{h}(.)$ are nonlinear in general.

It is assumed that the observations are taken at discrete time points Tk, with a discretisation time step T. The acceleration $\boldsymbol{u}_k$ of the mobile unit is usually highly correlated, but sometimes it undergoes rapid changes caused by various reasons such as traffic lights and road turns. Following [3], [7], [8], the motion of the moving user can be modeled as a dynamic system driven by a command $\boldsymbol{u}_k = (u_{x,k}, u_{y,k})'$ and a correlated random acceleration $\boldsymbol{r}_k = (r_{x,k}, r_{y,k})'$ at time k, i.e., the total acceleration is $\boldsymbol{a}_k = \boldsymbol{u}_k + \boldsymbol{r}_k$ (see Fig. 1).

III. Mobility State and Observation Models

Different state mobility models have previously been used in cellular networks such as the constant acceleration model [9] and Singer-type models [2], [4], [10]. In this paper we choose a discrete-time Singer-type model [7] because it captures correlated accelerations and allows for prediction of position, speed and acceleration of mobile users. Originally proposed in [11] for tracking targets in military systems, the Singer model has served as a basis for developing effective manoeuvre models for various applications (see [12] for a detailed survey), including user mobility patterns. In the original Singer model there is no control process and the acceleration is considered as a random process, which has a time autocorrelation. The Singer-type model from [2] includes a command process in explicit form. Yang and Wang consider a simpler form of this mobility model [7]. In our previous paper [13] we investigated the Singer-type model adopted for mobility tracking by [2]. However, we found that the model of [7] gives better results and at the same time is simpler since it enables a more efficient calculation of the PCRLBs. In this paper we adopt their model.

The state of the moving mobile at time instant k is defined by the vector $\boldsymbol{x}_k = (x_k, \dot{x}_k, \ddot{x}_k, y_k, \dot{y}_k, \ddot{y}_k)'$ where x_k and y_k specify the position, $\dot{x}_k$ and $\dot{y}_k$ specify the speed, and $\ddot{x}_k$ and $\ddot{y}_k$ specify the acceleration in the x and y directions in a two-dimensional space.

The motion of the mobility user can be described by the equation

$$\boldsymbol{x}_k = \boldsymbol{A}(T,\alpha)\boldsymbol{x}_{k-1} + \boldsymbol{B}_u(T)\boldsymbol{u}_k + \boldsymbol{B}_w(T)\boldsymbol{w}_k, \tag{3}$$

where $\boldsymbol{u}_k = (u_{x,k}, u_{y,k})'$ is a discrete-time command process and the respective matrices in (3) are of the form

$$\boldsymbol{A}(T,\alpha) = \begin{pmatrix} \tilde{\boldsymbol{A}} & \boldsymbol{0}_{3\times3} \\ \boldsymbol{0}_{3\times3} & \tilde{\boldsymbol{A}} \end{pmatrix}, \boldsymbol{B}_i(T) = \begin{pmatrix} \tilde{\boldsymbol{B}}_i & \boldsymbol{0}_{3\times1} \\ \boldsymbol{0}_{3\times1} & \tilde{\boldsymbol{B}}_i \end{pmatrix}, \tag{4}$$

$$\tilde{\boldsymbol{A}} = \begin{pmatrix} 1 & T & T^2/2 \\ 0 & 1 & T \\ 0 & 0 & \alpha \end{pmatrix}, \tilde{\boldsymbol{B}}_u = \begin{pmatrix} T^2/2 \\ T \\ 0 \end{pmatrix}, \tilde{\boldsymbol{B}}_w = \begin{pmatrix} T^2/2 \\ T \\ 1 \end{pmatrix}. \tag{5}$$

The subscript i in the matrix $\boldsymbol{B}(T)$ in (4) stands for u or w respectively. The random process $\boldsymbol{w}_k$ is a 2×1 vector, T is the discretisation period. The parameter α is the reciprocal of the manoeuvre time constant and thus depends on how long the manoeuvre lasts. Since $\boldsymbol{w}_k$ is a white noise, $E[\boldsymbol{w}_k\boldsymbol{w}'_{k+j}] = \boldsymbol{0}$, for $j \neq 0$. The covariance matrix $\boldsymbol{Q}$ of $\boldsymbol{w}_k$ is $\boldsymbol{Q} = \sigma_w^2\boldsymbol{I}$, where $\boldsymbol{I}$ denotes the unit matrix and σ_w is the standard deviation.

The unknown command processes $u_{x,k}$ and $u_{y,k}$ are modelled as a first-order Markov chain that takes values from a set of acceleration levels $\mathcal{M}_x$ and $\mathcal{M}_y$, and the process $\boldsymbol{u}_k$ takes values from the set $\mathbb{M} = \mathcal{M}_x \times \mathcal{M}_y = \{\boldsymbol{m}_1, \ldots, \boldsymbol{m}_M\}$, with transition probabilities $\boldsymbol{\pi}_{ij} = P(\boldsymbol{u}_k = \boldsymbol{m}_j | \boldsymbol{u}_{k-1} = \boldsymbol{m}_i)$, $i, j = 1, \ldots, M$ and initial probability distribution $\mu_{i,0} = P\{\boldsymbol{m} = \boldsymbol{m}_i\}$ for modes $\boldsymbol{m}_i \in \mathbb{M}$ such that $\mu_{i,0} \geq 0$ and $\sum_{i=1}^{M} \mu_{i,0} = 1$.

A. Observation Model

A commonly used model [2], [7] in cellular networks for the distance between a mobile and a given base station (BS) relies on the RSSI, which is the pilot signal strength received at the mobile. Denote by $z_{k,i}$ the RSSI signal received by a given mobile from the i-th BS with coordinates (a_i, b_i) at time k. The RSSI can be modelled as a sum of two terms: path loss and shadow fading. Fast fading is neglected assuming that a low-pass filter is used to attenuate the Rayleigh or Rician fade. Therefore, the RSSI (measured in dB) that the mobile unit receives from a particular BS i at time k can be modelled as the following function

$$z_{k,i} = z_{0,i} - 10\eta\log_{10}(d_{k,i}) + v_{k,i}, \tag{6}$$

where $z_{0,i}$ is a constant characterising the transmission power of the BS, depending on factors such as wavelength, antenna height and gain of cell i; η is a slope index (typically $\eta = 2$ for highways and $\eta = 4$ for microcells in a city); $d_{k,i} = \sqrt{(x_k - a_i)^2 + (y_k - b_i)^2}$ is the distance between the mobile unit and the base station; (a_i, b_i) is the position of the i-th BS; $v_{k,i}$ is the logarithm of the shadowing component, which was found in [3] to be a zero mean, stationary Gaussian process with standard deviation $\sigma_{v,i}$, typically from 4 – 8 dB. The shadowing component can considerably worsen the estimation process as it is shown in [2], [4]. This difficulty can be overcome by pre-filtering the measurements (e.g. by an averaging filter [2]) in order to reduce the observation noise.

To locate the mobile station (MS) in a two-dimensional plane, a minimum of three distance measurements to neighbouring BSs are sufficient to enable triangulation. Within the GSM system the MS is constantly monitoring up to 7 neighbouring BSs in order to establish the need for handovers. For the considered problem the observation vector consists of the three largest RSSI denoted $z_{k,1}, z_{k,2}, z_{k,3}$. Hence, the measurement equation is of the form

$$\boldsymbol{z}_k = \boldsymbol{h}(\boldsymbol{x}_k) + \boldsymbol{v}_k, \tag{7}$$

with $\boldsymbol{h}(\boldsymbol{x}_k) = (h_1(\boldsymbol{x}_k), h_2(\boldsymbol{x}_k), h_3(\boldsymbol{x}_k))'$, $h_i(x_{i,k}) = z_{0,i} - 10\eta\log(d_{k,i})$, a measurement vector $\boldsymbol{z}_k = (z_{k,1}, z_{k,2}, z_{k,3})'$, shadowing components $\boldsymbol{v}_k = (v_{k,1}, v_{k,2}, v_{k,3})'$ assumed to be uncorrelated both in time and space and having Gaussian distribution, $v_{k,i} = \mathcal{N}(0, \sigma^2_{v,i})$.

IV. Mobility Tracking and Prediction within Bayesian Framework

We now consider the sequential estimation of the mobility of a user within the Bayesian framework. Since the command process $\boldsymbol{u}$ is unknown, we are considering a hybrid particle $\mathbf{x}_k = (\boldsymbol{x}'_k, \boldsymbol{m}'_k)'$ that fully characterises the target state and mode. The mobility state $\mathbf{x}_k$ can be evaluated at each time instant from the conditional probability density function $p(\mathbf{x}_k|\boldsymbol{z}_{1:k})$ and a set of measurements $\boldsymbol{z}_{1:k} \triangleq \{\boldsymbol{z}_1, \ldots, \boldsymbol{z}_k\}$ up to time instant k via the Chapman-Kolmogorov equation

$$p(\mathbf{x}_k|\boldsymbol{z}_{1:k-1}) = \int_{\mathbb{R}^{n_x}} p(\mathbf{x}_k|\mathbf{x}_{k-1}) p(\mathbf{x}_{k-1}|\boldsymbol{z}_{1:k-1}) d\mathbf{x}_{k-1}. \tag{8}$$

After the arrival of the measurement $\boldsymbol{z}_k$ at time k, the posterior state probability density function (pdf) can be updated via Bayes rule

$$p(\mathbf{x}_k|\boldsymbol{z}_{1:k}) = \frac{p(\boldsymbol{z}_k|\mathbf{x}_k) p(\mathbf{x}_k|\boldsymbol{z}_{1:k-1})}{p(\boldsymbol{z}_k|\boldsymbol{z}_{1:k-1})}, \tag{9}$$

where $p(\boldsymbol{z}_k|\boldsymbol{z}_{1:k-1})$ is a normalising constant. The analytical solution to the above equations is intractable. Hence, we utilise the MC technique [14] which has proven to be very suitable and powerful for dealing with nonlinear system dynamics.

The MC approach relies on a sample-based construction of these probability density functions. Multiple particles (samples) of the variables of interest are generated, each one associated with a weight which characterises the belief that the object is in this state. An estimate of the variable of interest is obtained by the weighted sum of particles. Two major stages can be distinguished: *prediction* and *update*. During the prediction each particle is modified according to the state model, including the addition of random noise in order to simulate the effect of the noise on the variable of interest. Then in the update stage, each particle's weight is re-evaluated based on the new sensor data. A *resampling* procedure is dealing with the elimination of particles with small weights and replicates the particles with higher weights.

A. A Particle Filter for Mobility Tracking

The developed particle filter (PF) is based on multiple models for the unknown acceleration $\boldsymbol{u}$. A detailed scheme of the PF is given below, where N denotes the number of particles.

A particle filter for mobility tracking

Initialisation

I. $k = 0$, for $j = 1, \ldots, N$,
generate samples $\{\boldsymbol{x}_0^{(j)} \sim p(\boldsymbol{x}_0), \boldsymbol{m}_0^{(j)} \sim P_0(\boldsymbol{m})\}$,
where $P_0(\boldsymbol{m})$ are the initial mode probabilities for the accelerations and set initial weights $W^{(j)} = 1/N$.

II. For $k = 1, 2, \ldots,$

1) *Prediction Step*
For $j = 1, \ldots, N$, generate samples

$$\boldsymbol{x}_k^{(j)} = \boldsymbol{A}(T, \alpha)\boldsymbol{x}_{k-1}^{(j)} + \boldsymbol{B}_u(T)\boldsymbol{u}^{(j)}(\boldsymbol{m}_k^{(j)}) + \boldsymbol{B}_w(T)\boldsymbol{w}_k^{(j)},$$

where $\boldsymbol{w}_k^{(j)} \sim \mathcal{N}(\boldsymbol{0}, \boldsymbol{Q})$, and under the constraint:

$$\text{if } V = \sqrt{(\dot{x}_k^{(j)})^2 + (\dot{y}_k^{(j)})^2} > V_{\max}, \tag{10}$$

$\alpha_c = \arctan\{\dot{y}_k^{(j)}/\dot{x}_k^{(j)}\}$,
$\dot{x}_k^{(j)} = V_{\max}\cos(\alpha_c), \ \ \dot{y}_k^{(j)} = V_{\max}\sin(\alpha_c)$,
end

$\boldsymbol{m}_k^{(j)} \sim \{\boldsymbol{\pi}_{\ell m}\}_{m=1}^{M}, \ m = 1, \ldots, M \ \text{ for } \ \ell = \boldsymbol{m}_{k-1}^{(j)};$

Measurement Update: evaluate the importance weights

2) for $j = 1, \ldots, N$, on the receipt of a new measurement, compute the weights

$$W_k^{(j)} = W_{k-1}^{(j)} \mathcal{L}(\boldsymbol{z}_k|\boldsymbol{x}_k^{(j)}). \tag{11}$$

The likelihood $\mathcal{L}(\boldsymbol{z}_k|\boldsymbol{x}_k^{(j)})$ is calculated using (7) $\mathcal{L}(\boldsymbol{z}_k|\boldsymbol{x}_k^{(j)}) \sim \mathcal{N}(\boldsymbol{h}(\boldsymbol{x}_k^{(j)}), \sigma_v)$.

3) for $j = 1, \ldots, N$, normalise the weights,
$\hat{W}_k^{(j)} = W_k^{(j)} / \sum_{j=1}^{N} W_k^{(j)}$.

Output

4) The posterior mean $E[\boldsymbol{x}_k|\boldsymbol{z}_{1:k}]$

$$\hat{\boldsymbol{x}}_k = E[\boldsymbol{x}_k|\boldsymbol{z}_{1:k}] = \sum_{j=1}^{N} \hat{W}_k^{(j)} \boldsymbol{x}_k^{(j)}. \tag{12}$$

Calculate posterior mode probabilities

5) for $j = 1, \ldots, N$,
$P(\boldsymbol{m}_k = \ell|\boldsymbol{z}_{1:k}) = \sum_{j=1}^{N} 1(\boldsymbol{m}_k^{(j)} = \ell)\hat{W}_k^{(j)}$,
where $1(.)$ is an indicator function such that

$$1(\boldsymbol{m}_k) = \begin{cases} 1, & \text{if } \boldsymbol{m}_k = \ell; \\ 0, & \text{otherwise.} \end{cases}$$

Compute the effective sample size

6) $N_{eff} = 1/\sum_{j=1}^{N}(\hat{W}_k^{(j)})^2$,

Selection step (resampling) if $N_{eff} < N_{thresh}$

7) Multiply/ suppress samples $\{\boldsymbol{x}_k^{(j)}, \boldsymbol{m}_k^{(j)}\}$ with high/ low importance weights $\hat{W}_k^{(j)}$, in order to obtain N new random samples approximately distributed according to the posterior state distribution. The residual resampling algorithm [15], [16] is applied. This is a two step process making use of sampling-importance-resampling scheme.
* For $j = 1, \ldots, N$, set $W_k^{(j)} = \hat{W}_k^{(j)} = 1/N$.

The PF takes into account the fact that the speed of the mobile unit cannot exceed certain values (Eq. (10)). Other refined schemes for accounting for constraints can also be applied [17].

V. A Rao-Blackwellised Particle Filter for Mobility Tracking

A major drawback of particle filtering is that it can become prohibitively expensive when a large number of particles is used. However, the complexity can be reduced by a procedure called Rao-Blackwellisation [17]–[23].

Rao-Blackwellisation is a technique for improving particle filtering by analytically marginalising some of the variables (linear, Gaussian) from the joint posterior distribution. The linear part of the system model is then estimated by a Kalman filter (KF), an optimal estimator, whilst the nonlinear part is estimated by a PF. This leads to the fact that a KF is attached to each particle. In the mobility tracking problem the positions of the mobile unit are estimated with a PF, whilst the speeds and accelerations with a KF. Since the measurement equation is highly nonlinear, the particle filter is used to approximate this distribution. After estimating the positions, these estimates are given to the KF as measurements. As a result of the marginalisation, the variance of the estimates can be reduced compared with the standard PF.

Similarly to the Rao-Blackwellisation approach, the mixture Kalman filtering approach proposed by Chen and Liu [24] represents the system in a linear conditional dynamic model. In this way the problem is solved by multiple Kalman filters run with the MC sampling approach. A formulation of the Rao-Blackwellisation problem is given in [25], [26] in a way different from that in [20]. In the implementation of our Rao-Blackwellised PF for mobility tracking we follow the approach proposed in [19] and [20]. In contrast to these works we design a RBPF which has a command process in the system model.

The mobility model (1)-(2) is rewritten in the form

$$\begin{pmatrix} \boldsymbol{x}_k^{pf} \\ \boldsymbol{x}_k^{kf} \end{pmatrix} = \begin{pmatrix} \boldsymbol{I} & \boldsymbol{A}^{pf} \\ \boldsymbol{0} & \boldsymbol{A}^{kf} \end{pmatrix} \begin{pmatrix} \boldsymbol{x}_{k-1}^{pf} \\ \boldsymbol{x}_{k-1}^{kf} \end{pmatrix} + \begin{pmatrix} \boldsymbol{B}_u^{pf} \\ \boldsymbol{B}_u^{kf} \end{pmatrix} \boldsymbol{u}_k + \begin{pmatrix} \boldsymbol{B}_w^{pf} \\ \boldsymbol{B}_w^{kf} \end{pmatrix} \boldsymbol{w}_k, \tag{13}$$

$$\boldsymbol{z}_k = \boldsymbol{h}(\boldsymbol{x}_k^{pf}) + \boldsymbol{v}_k, \tag{14}$$

where $\boldsymbol{x}^{pf} = (x, y)'$, 'pf' is short for particle filter, $\boldsymbol{x}^{kf} = (\dot{x}, \ddot{x}, \dot{y}, \ddot{y})'$, 'kf' is short for Kalman filter and $\boldsymbol{w}$ is assumed Gaussian. Equations (13)-(14) have the same properties as equations (1)-(2). Since the noise $\boldsymbol{w}_k$ is Gaussian,

$$\boldsymbol{w}_k = \begin{pmatrix} \boldsymbol{w}_k^{pf} \\ \boldsymbol{w}_k^{kf} \end{pmatrix} \in \mathcal{N} \sim (\boldsymbol{0}, \boldsymbol{Q}), \boldsymbol{Q} = \begin{pmatrix} \boldsymbol{Q}^{pf} & \boldsymbol{M} \\ \boldsymbol{M}' & \boldsymbol{Q}^{kf} \end{pmatrix}, \tag{15}$$

The mobility model is a Singer-type model which accounts for correlations between the state vector components. Hence, we cannot assume that the process noise $\boldsymbol{w}^{pf}$ is uncorrelated with $\boldsymbol{w}^{kf}$, i.e. $\boldsymbol{M} \neq \boldsymbol{0}$.

Instead of directly estimating the pdf $p(\boldsymbol{x}_k|\boldsymbol{z}_{1:k})$, with the entire state vector, consider the pdf $p(\boldsymbol{x}_k^{pf}, \boldsymbol{x}_k^{kf}|\boldsymbol{z}_{1:k})$. Using the Bayes rule, this pdf can be factorised into two parts

$$p(\boldsymbol{x}_k^{pf}, \boldsymbol{x}_k^{kf}|\boldsymbol{z}_{1:k}) = p(\boldsymbol{x}_k^{kf}|\boldsymbol{x}_k^{pf}, \boldsymbol{z}_{1:k}) p(\boldsymbol{x}^{pf}|\boldsymbol{z}_{1:k}). \tag{16}$$

Since the measurements $\boldsymbol{z}_{1:k}$ are conditionally independent on $\boldsymbol{x}_k^{kf}$, the probability $p(\boldsymbol{x}_k^{kf}|\boldsymbol{x}_k^{pf}, \boldsymbol{z}_{1:k})$ can be written as

$$p(\boldsymbol{x}_k^{kf}|\boldsymbol{x}_k^{pf}, \boldsymbol{z}_{1:k}) = p(\boldsymbol{x}_k^{kf}|\boldsymbol{x}_k^{pf}). \tag{17}$$

Consider now the system

$$\begin{aligned} \boldsymbol{x}_k^{kf} &= \boldsymbol{A}^{kf}\boldsymbol{x}_{k-1}^{kf} + \boldsymbol{B}_u^{kf}\boldsymbol{u}_k + \boldsymbol{B}_w^{kf}\boldsymbol{w}_k^{kf}, \\ \boldsymbol{z}_k &= \boldsymbol{A}^{pf}\boldsymbol{x}_{k-1}^{kf} + \boldsymbol{B}_u^{pf}\boldsymbol{u}_k + \boldsymbol{B}_w^{pf}\boldsymbol{w}_k^{pf}, \end{aligned} \tag{18}$$

where $\boldsymbol{z}_k = \boldsymbol{x}_k^{pf} - f(\boldsymbol{x}_k^{pf})$. Since the system (18) is linear and Gaussian, the optimal solution is provided by the KF. We can assume a Gaussian form of the pdf (17), i.e.

$$p(\boldsymbol{x}_k^{kf}|\boldsymbol{x}_k^{pf}) \sim \mathcal{N}(\hat{\boldsymbol{x}}_{k|k-1}^{kf}, \boldsymbol{P}_{k|k-1}^{kf}), \tag{19}$$

where the estimate vector $\hat{\boldsymbol{x}}_{k|k-1}^{kf}$ and the corresponding covariance matrix $\boldsymbol{P}_{k|k-1}^{kf}$ are calculated by the Kalman filter.

The second pdf from (16) can be written recursively [19]

$$p(\boldsymbol{x}_k^{pf}|\boldsymbol{z}_{1:k}) = \frac{p(\boldsymbol{z}_k|\boldsymbol{x}_k^{pf})p(\boldsymbol{x}_k^{pf}|\boldsymbol{x}_{1:k-1}^{pf})}{p(\boldsymbol{z}_k|\boldsymbol{z}_{1:k-1})} p(\boldsymbol{x}_{1:k-1}^{pf}|\boldsymbol{z}_{1:k-1}). \tag{20}$$

Due to the nonlinear measurement equation we apply a PF to solve (20). The weights are recursively calculated based on the likelihoods $p(\boldsymbol{z}_k|\boldsymbol{x}_k^{pf,(j)})$. The particles will be sampled according to $p(\boldsymbol{x}_k^{pf,(j)}|\boldsymbol{x}_{1:k-1}^{pf,(j)})$. Using the state equation for the $\boldsymbol{x}^{pf}$ from (13) and having in mind (19), the prediction step in the particle filter can be performed as follows

$$\begin{aligned} \boldsymbol{x}_{k+1}^{pf,(j)} \sim \mathcal{N}(&\boldsymbol{x}_k^{pf,(j)} + \boldsymbol{A}^{pf}\hat{\boldsymbol{x}}_{k|k-1}^{kf,(j)} + \boldsymbol{B}_u^{pf}\boldsymbol{u}_{k+1}^{(j)}, \\ &\boldsymbol{A}^{pf}\boldsymbol{P}_{k|k-1}^{kf,(j)}(\boldsymbol{A}^{pf})' + \boldsymbol{B}_w^{pf}\boldsymbol{Q}^{pf}(\boldsymbol{B}_w^{pf})'. \end{aligned} \tag{21}$$

For each particle, one Kalman filter estimates $\boldsymbol{x}_{k+1|k}^{kf,(j)}$, $j = 1,\dots,N$. It should be noted that the prediction of the nonlinear variables is used to improve the estimates of the linear state variables.

Next, we present the developed RBPF. Note that in the KF update and prediction steps, the filter gain $\boldsymbol{K}_k$, the predicted and estimated covariance matrices, $\boldsymbol{P}_{k|k}^{kf}$, $\boldsymbol{P}_{k-1|k}^{kf}$ are calculated once, which reduces the computational load.

A Rao-Blackwellised PF for mobility tracking

Initialisation

1) $k = 0$, for $j = 1,\dots,N$, generate samples $\{\boldsymbol{x}_0^{pf,(j)} \sim p(\boldsymbol{x}_0^{pf}), \boldsymbol{m}_0^{(j)} \sim P_0(\boldsymbol{m})\}$, where $P_0(\boldsymbol{m})$ are the initial mode probabilities for the accelerations. Initialise the Kalman filters by $\{\hat{\boldsymbol{x}}_{0|-1}^{kf,(j)} \sim \mathcal{N}\left(\hat{\boldsymbol{x}}_{0|-1}^{kf}, \boldsymbol{P}_{0|-1}^{kf}\right)\}$ and set initial weights $W_0^{(j)} = 1/N$.

Particle Filter Prediction Step

2) For $j = 1,\dots,N$, Predict the particles

$$\boldsymbol{x}_{k+1}^{pf,(j)} = \mathcal{N}(\boldsymbol{x}_k^{pf,(j)} + \boldsymbol{A}^{pf}\boldsymbol{x}_{k|k-1}^{kf,(j)} + \boldsymbol{B}_u^{pf}\boldsymbol{u}(\boldsymbol{m}_{k+1}^{(j)}),\\ \boldsymbol{A}^{pf}\boldsymbol{P}_{k|k-1}^{kf}(\boldsymbol{A}^{pf})^T + \boldsymbol{B}_w^{pf}\boldsymbol{Q}_w^{pf}(\boldsymbol{B}_w^{pf})'), \quad (22)$$

where $\boldsymbol{m}_{k+1}^{(j)} \sim \{\pi_{\ell m}\}_{m=1}^{M}$ for $\ell = \boldsymbol{m}_k^{(j)}$;

3) *Update step of the Kalman filters*

$$\boldsymbol{K}_k = \boldsymbol{P}_{k|k-1}^{kf}(\boldsymbol{A}^{pf})'(\boldsymbol{S}_k)^{-1}, \quad (23)$$

$$\boldsymbol{P}_{k|k}^{kf} = \boldsymbol{P}_{k|k-1}^{kf} - \boldsymbol{K}_k\boldsymbol{A}^{pf}\boldsymbol{P}_{k|k-1}^{kf}, \quad (24)$$

$$\boldsymbol{S}_k = \boldsymbol{A}^{pf}\boldsymbol{P}_{k|k-1}^{kf}(\boldsymbol{A}^{pf})' + \boldsymbol{B}_w^{pf}\boldsymbol{Q}^{pf}(\boldsymbol{B}_w^{pf})', \quad (25)$$

For $j = 1,2,\dots,N$

$$\boldsymbol{x}_{k|k}^{kf,(j)} = \boldsymbol{x}_{k|k-1}^{kf,(j)} + \boldsymbol{K}_k(\boldsymbol{z}_k^{(j)} - \boldsymbol{A}^{pf}\hat{\boldsymbol{x}}_{k|k-1}^{kf,(j)}), \quad (26)$$

where $\boldsymbol{z}_k^{(j)} = \boldsymbol{x}_{k+1}^{pf,(j)} - \boldsymbol{x}_k^{pf,(j)}$ and under the constraint:

$$\text{if } V = \sqrt{(\hat{\dot{x}}_{k|k}^{(j)})^2 + (\hat{\dot{y}}_{k|k}^{(j)})^2} > V_{\max}, \quad (27)$$

$$\alpha_c = \arctan\{\hat{\dot{y}}_{k|k}^{(j)}/\hat{\dot{x}}_{k|k}^{(j)}\},$$
$$\hat{\dot{x}}_{k|k}^{(j)} = V_{\max}\cos(\alpha_c),\ \hat{\dot{y}}_{k|k}^{(j)} = V_{\max}\sin(\alpha_c),$$

end

4) *Prediction step of the Kalman filters*

$$\boldsymbol{P}_{k+1|k}^{kf} = \boldsymbol{D}\boldsymbol{P}_{k|k}^{kf}\boldsymbol{D}' + \boldsymbol{B}_w^{kf}\bar{\boldsymbol{Q}}^{kf}(\boldsymbol{B}_w^{kf})', \quad (28)$$

where

$$\boldsymbol{C} = \boldsymbol{M}'(\boldsymbol{Q}^{pf})^{-1}, \quad (29)$$

$$\boldsymbol{D} = \boldsymbol{A}^{kf} - \boldsymbol{C}\boldsymbol{A}^{pf}, \quad (30)$$

$$\bar{\boldsymbol{Q}}^{kf} = \boldsymbol{Q}^{kf} - \boldsymbol{M}'(\boldsymbol{Q}^{pf})^{-1}\boldsymbol{M}, \quad (31)$$

For $j = 1,2,\dots,N$

$$\boldsymbol{x}_{k+1|k}^{kf,(j)} = \boldsymbol{D}\hat{\boldsymbol{x}}_{k|k}^{kf,(j)} + \boldsymbol{C}\boldsymbol{z}_k^{(j)} + \boldsymbol{B}_u^{kf}\boldsymbol{u}(\boldsymbol{m}_{k+1}^{(j)}). \quad (32)$$

Measurement Update: evaluate the importance weights

5) Compute the weights

$$W_{k+1}^{(j)} = W_k^{(j)}\mathcal{L}(\boldsymbol{z}_{k+1}|\boldsymbol{x}_{k+1}^{pf,(j)}). \quad (33)$$

The likelihood $\mathcal{L}(\boldsymbol{z}_{k+1}|\boldsymbol{x}_{k+1}^{pf,(j)})$ is calculated from (7) $\mathcal{L}(\boldsymbol{z}_{k+1}|\boldsymbol{x}_{k+1}^{pf,(j)}) \sim \mathcal{N}(\boldsymbol{h}(\boldsymbol{x}_{k+1}^{pf,(j)}), \sigma_v)$.

6) Normalise weights, $\hat{W}_{k+1}^{(j)} = W_{k+1}^{(j)}/\sum_{j=1}^{N} W_{k+1}^{(j)}$.

7) *Output*

$$\hat{\boldsymbol{x}}_{k+1}^{pf} \approx \sum_{j=1}^{N}\hat{W}_{k+1}^{(j)}\boldsymbol{x}_{k+1}^{pf,(j)}, \quad (34)$$

$$\hat{\boldsymbol{x}}_{k+1}^{kf} \approx \sum_{j=1}^{N}\hat{W}_{k+1}^{(j)}\hat{\boldsymbol{x}}_{k+1|k}^{kf,(j)}, \quad (35)$$

Calculate posterior mode probabilities

8) $P(\boldsymbol{m}_{k+1} = \ell|\boldsymbol{z}_{1:k+1}) = \sum_{j=1}^{N} 1(\boldsymbol{m}_{k+1}^{(j)} = \ell)\hat{W}_{k+1}^{(j)}$, where $1(.)$ is an indicator function such that

$$1(\boldsymbol{m}_k) = \begin{cases} 1, & \text{if } \boldsymbol{m}_k = \ell; \\ 0, & \text{otherwise.} \end{cases}$$

Selection step (resampling)

9) If $N_{eff} < N_{thresh}$ resample $\{\boldsymbol{x}_{k+1}^{pf,(j)},\ \boldsymbol{x}_{k+1/k}^{kf,(j)}, \boldsymbol{m}_{k+1}^{(j)}\}$ in the same way as in the PF.

10) Set $k = k+1$ and return to step 2.

A. Mobility Prediction

Based on the approximation of the filtering distribution $p(\mathbf{x}_k|\boldsymbol{z}_{1:k})$ we seek to estimate the t-step ahead prediction distribution ($t \geq 2$). In a general prediction problem we are interested in computing the posterior t-step ahead prediction distribution $p(\mathbf{x}_{k+r}|\boldsymbol{z}_{1:k})$ given by [7], [25]

$$p(\mathbf{x}_{k+t}|\boldsymbol{z}_{1:k}) = \int_{\mathbb{R}^{n_x}} p(\mathbf{x}_k|\boldsymbol{z}_{1:k})\left[\prod_{i=k+1}^{k+t} d\mathbf{x}_{k:k+t-1}\right], \quad (36)$$

where $\mathbf{x}_{k+t} = \{\boldsymbol{x}_k, \boldsymbol{u}_k, \dots, \boldsymbol{x}_{k+t}, \boldsymbol{u}_{k+t}\}$. Then the solution to the t step ahead prediction can be given by performing the following steps.

r step ahead prediction

* For $i = 1,\dots,t$, For $j = 1,2,\dots,N$, sample
$\boldsymbol{x}_{k+i}^{(j)} = \boldsymbol{A}(T,\alpha)\boldsymbol{x}_{k+i-1}^{(j)} + \boldsymbol{B}_u(T)\boldsymbol{u}^{(j)}(\boldsymbol{m}_{k+i}) + \boldsymbol{B}_w(T)\boldsymbol{w}_{k+i}^{(j)}$,
where $\boldsymbol{w}_{k+i}^{(j)} \sim \mathcal{N}(\boldsymbol{0}, \boldsymbol{Q})$,
$\boldsymbol{m}_{k+i}^{(j)} \sim \{\pi_{\ell m}\}_{\ell=1}^{M},\ m = 1,\dots,M$ for $\ell = \boldsymbol{m}_{k+i-1}^{(j)}$;

Then the predicted state estimate of the mobile unit is equal to

$$\hat{\boldsymbol{x}}_{k+t/k} = \sum_{j=1}^{N_{mc}} W_k^{(j)}\boldsymbol{x}_{k+t|k}^{(j)}. \quad (37)$$

VI. Posterior Cramér-Rao Lower Bound (PCRLB)

The posterior CRLB (PCRLB) [17], [27], [28] characterises the best achievable theoretical accuracy in nonlinear filtering. This is of paramount importance for assessing the level of approximation introduced by the algorithms.

Consider a sequence of target states (a trajectory) $\boldsymbol{X}_k = \{\boldsymbol{x}_1, \boldsymbol{x}_2, \ldots, \boldsymbol{x}_k\}$ estimated based on the set of measurements $\boldsymbol{z}_{1:k}$. Since the hybrid estimation problem deals with joint estimation of the state vector $\boldsymbol{x}_k$ and the mode variable $\boldsymbol{m}_k$, the PCRLB is the inverse $\boldsymbol{J}_k$ of the information matrix and is defined as follows [29]

$$\boldsymbol{J}_k \triangleq E\{[\nabla_{\mathbf{Y}_k} \log\, p(\mathbf{Y}_k, \boldsymbol{z}_{1:k})][\nabla_{\mathbf{Y}_k} \log\, p(\mathbf{Y}_k, \boldsymbol{z}_{1:k})]'\}, \tag{38}$$

where $\mathbf{Y}_k = [\mathbf{X}_k, \mathbb{M}_k]'$, with $\mathbb{M}_k = \{\boldsymbol{m}_1, \ldots, \boldsymbol{m}_M\}$ being the random regime sequence; $\nabla_{\mathbf{Y}_k}$ is the first-order partial derivative operator with respect to $\mathbf{Y}_k$. The analytical derivation of the PCRLB for hybrid state estimation is a difficult problem. In the derivation of the PCRLB we follow the approach from [17] (Ch. 4, p. 76).

When the target trajectory is generated in a deterministic way and the sequence of modes is deterministic, then the PCRLB is identical to the covariance matrix propagation of the Extended Kalman Filter (EKF) with Jacobians evaluated at the true state vector $\boldsymbol{x}_k$ and true regimes. This is a very "optimistic" bound. This bound is often calculated in practice [17] and most tracking system specifications consider purely deterministic trajectories. In our work we also calculate the PCRLB for a deterministic trajectory. If the target trajectory is deterministic, but the sequence of modes is random, the PCRLB can be calculated in a similar way [17].

VII. Performance Evaluation

Example 1. The developed MC algorithms have been evaluated over a conventional hexagonal cellular network (similar to those in [7]). It is supposed that a map of the cellular network is available and the centre coordinates of the base stations are known. The simulated service area contains 64 base stations with cell radius of 2 km, as shown in Fig. 2. The mobile can move to any cell of the network with varying speed and acceleration. The sequence of modes in the testing scenario is generated in a deterministic way. Short-time manoeuvres are followed by uniform motions. The discrete-time command processes $u_{x,k}$ and $u_{y,k}$ can change within the range $[-5, 5]$ $[m/s^2]$. The command process $\boldsymbol{u}_k$ in the filters is assumed to be a Markov chain, taking values between the following acceleration levels $\mathbb{M} = M_x \times M_y = \{(0.0, 0.0),\ (3.5, 0.0),\ (0.0, 3.5),\ (0.0, -3.5),\ (-3.5, 0.0)\}$, in units of $[m/s^2]$. The simulated trajectory of the mobile is generated deterministically according to the mobility model (3) and, with this trajectory, the RSSI signals are randomly generated according to the observation equation (7) with different random noise realisations for each simulation run. The randomness of the RSSI comes from the randomness of the shadowing component. At any sampling time, the observed RSSI signal is chosen to be the three largest signal powers among all 64 BSs in the network. The simulation parameters are summarised in *Table 1*.

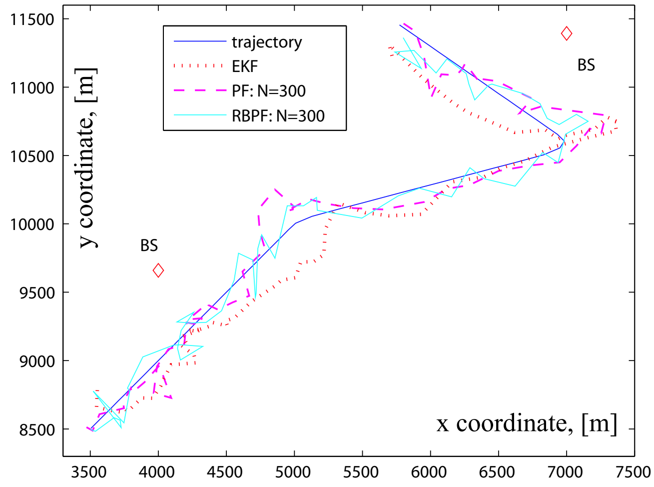

Fig. 2. Centres of the base stations, the actual trajectory of the mobile unit, estimated trajectories by the EKF, PF and RBPF from a single realisation.

After partitioning the state vector according to (13) within the RBPF scheme the respective matrices of the PF and KF acquire the form:

$$\boldsymbol{A}^{pf} = \begin{pmatrix} T & T^2/2 & 0 & 0 \\ 0 & 0 & T & T^2/2 \end{pmatrix}, \boldsymbol{B}_u^{pf} = \begin{pmatrix} T^2/2 & 0 \\ 0 & T^2/2 \end{pmatrix},$$

$$\boldsymbol{Q}^{pf} = \begin{pmatrix} q_{11} & 0 \\ 0 & q_{11} \end{pmatrix} \sigma_w^2,\ \boldsymbol{M}^{pf} = \begin{pmatrix} q_{12} & q_{13} & 0 & 0 \\ 0 & 0 & q_{12} & q_{13} \end{pmatrix},$$

$$\boldsymbol{A}^{kf} = \begin{pmatrix} 1 & T & 0 & 0 \\ 0 & \alpha & 0 & 0 \\ 0 & 0 & 1 & T \\ 0 & 0 & 0 & \alpha \end{pmatrix}, \boldsymbol{B}_u^{kf} = \begin{pmatrix} T & 0 \\ 0 & 0 \\ 0 & T \\ 0 & 0 \end{pmatrix},$$

$$\boldsymbol{B}_w^{kf} = \begin{pmatrix} T & 0 \\ 1 & 0 \\ 0 & T \\ 0 & 1 \end{pmatrix},\quad \boldsymbol{Q}^{kf} = \begin{pmatrix} q_{22} & q_{23} & 0 & 0 \\ q_{23} & q_{33} & 0 & 0 \\ 0 & 0 & q_{22} & q_{23} \\ 0 & 0 & q_{33} & q_{33} \end{pmatrix} \sigma_w^2,$$

$$\boldsymbol{B}_w^{pf} = \boldsymbol{B}_u^{pf},$$

where $q_{ij},\quad i, j = 1, 2, 3$ have the form $q_{11} = T^4/4$, $q_{12} = T^3/2$, $q_{13} = T^2/2$, $q_{22} = T^2$, $q_{23} = T$, $q_{33} = 1$.

Table 1. Simulation parameters

Discretisation time step T	0.5 [s]
Correlation coefficient α	0.6
Path loss index η	3
Base station transmission power $z_{0,i}$	90
Covariance σ_w^2 of the noise $\boldsymbol{w}_k$ in (3)	0.5^2 $[m/s^2]^2$
Maximum speed $V_{\max}$	45 $[m/s]$
Transition probabilities $p_{i,i}$	0.8
Initial mode probabilities $\mu_{i,0}$	$1/M,\ i = 1, ..., M,\ M = 5$
Threshold for resampling	$N_{thresh} = N/10$
Number of Monte Carlo runs	$N_{mc} = 100$
Covariance σ_v^2 of the noise $v_{i,k}$	$[4^2]$ [dB]^2

The estimated and actual trajectories of the mobile unit over a single realisation are given in Fig. 2.

The position root-mean-square error (RMSE) [30]

$$RMSE = \sqrt{\frac{1}{N_{mc}} \sum_{m=1}^{N_{mc}} [(\hat{x}_k - x_k)^2 + (\hat{y}_k - y_k)^2]} \tag{39}$$

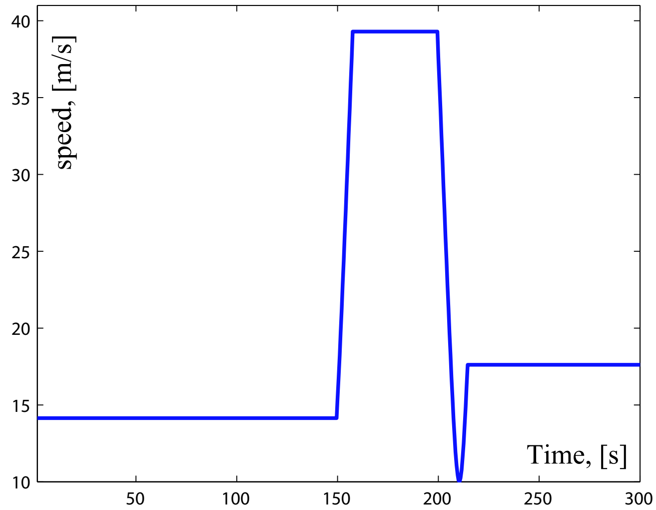

Fig. 3. Actual speed of the moving unit. This figure shows the abrupt manoeuvre in the MS motion.

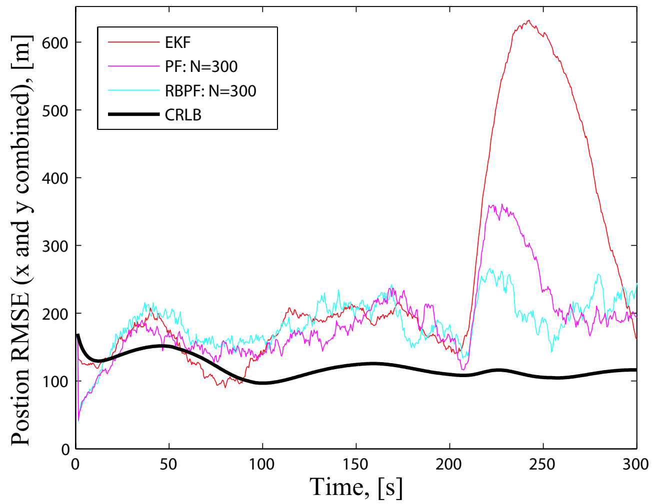

Fig. 4. RMSE of x and y positions combined of the EKF, PF and RBPF for $N_{mc} = 100$ runs. The PF and RBPF particles are N = 300.

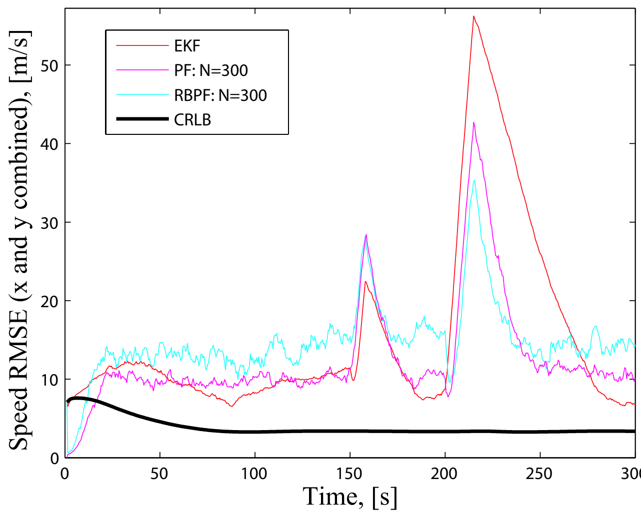

Fig. 5. RMSE of $\dot{x}$ and $\dot{y}$ speeds combined of the EKF, PF and RBPF (with N = 300) for $N_{mc} = 100$ runs.

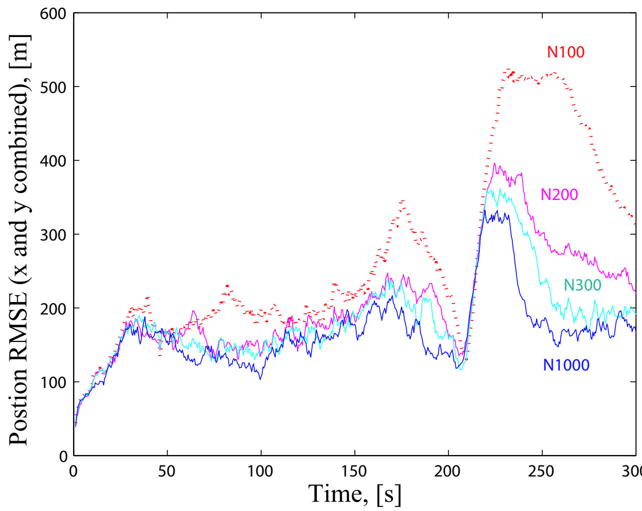

Fig. 6. PF Position RMSE (x and y combined) of the PF with $N = 100,\ 200, 300$ and 1000.

is used to assess the closeness of the estimated trajectory $\{\hat{x}_k, \hat{y}_k\}$ to a given trajectory $\{x_k, y_k\}$ over $N_{mc} = 100$ MC runs. The location PCRLB is determined as

$$location\ PCRLB = \sqrt{(\boldsymbol{P}_k(1,1) + \boldsymbol{P}_k(4,4))}, \tag{40}$$

where $\boldsymbol{P}$ is the covariance matrix of the EKF having Jacobians evaluated for the true state vector $\boldsymbol{x}_k$.

Figures 4-5 present the position and speed RMSE of the PF and RBPF, respectively, with N =300 particles. The RBPF and PF outperform the EKF. This is very pronounced during the manoeuvres where the EKF peak dynamic errors are the highest. Figures 6-9 presents results from the PF and RBPF with a different number of particles. The position RMSE of the PF increases with $N = 100$ compared with the case with $N = 500$ (Figures 6-7). The RBPF, on the other hand exhibits very good performance with a small number of particles (Figures 8-9, $N = 200$) which is his advantage.

The trade-off between accuracy and complexity is an important issue and for marginalised PFs has been analysed in [31]. On average, for these 100 Monte Carlo runs, when the PF is working with $N = 500$ particles, and the RBPF with 200 particles, the average computational time of the RBPF is reduced by 60% compared with the PF. If the RBPF operates with 100 particles, the reduction of its computational time compared with the PF with $N = 500$ is more than 70% with reduced accuracy.

In conclusion, the developed RBPF has similar accuracy to the PF with respect to the position and speed, with decreased computational time when we use a small number of particles, e.g., $N = 200$. The PF accuracy is worsen when $N < 500$.

Figure 10 shows the accuracy of the algorithms for different numbers of particles and the average computational time for one cycle of the algorithms over 100 MC runs. It can be seen from the table, that position RMSEs of the RBPF with N=200 particles is nearly the same as the position RMS errors of the PF with N=300. Thus, a similar performance can be achieved by the RBPF with decreased computational resources.

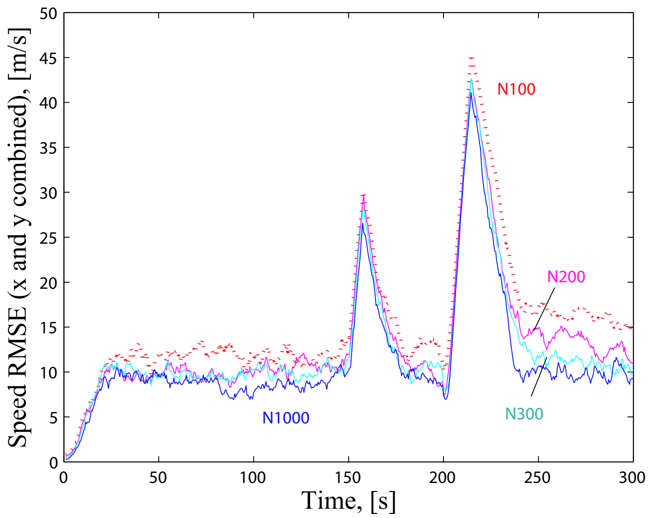

Fig. 7. RMSE of $\dot{x}$ and $\dot{y}$ speeds combined of the PF with $N = 100,\ 200, 300$ and 1000.

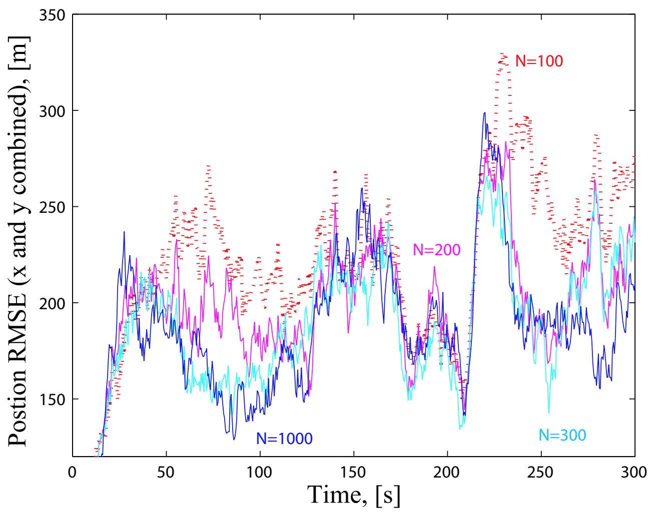

Fig. 8. Position RMSE (x and y combined) of the RBPF with $N = 100,\ 200, 300, 500$ and 1000.

Example 2. The performance of the mobility tracking algorithms has been investigated with real RSSIs, collected from BSs in Glasgow, United Kingdom. The mobile station was a vehicle driving in the city centre. More than 400 BSs are available in the area where the car operated. However, only data from the six with the highest RSSIs were provided to the algorithms. Figure 11 presents the map of the urban environment, with the nearest base stations and the trajectory of the car (shown augmented in Figure 12). The vehicle trajectory contains both patterns with sharp manoeuvres and rectilinear motion, including a stretch at the end where the vehicle is parked. Additional information for the road is included as position constraints in the algorithms. The MC algorithms have shown efficiency in all these conditions. Apart from the signal strengths, a GPS system collected the actual positions of the moving MS, with the sampling period, $T = 0.5\ s$. Figure 13 shows the actual MS trajectory together with the estimated trajectories and Figure 14 gives the respective position RMSEs.

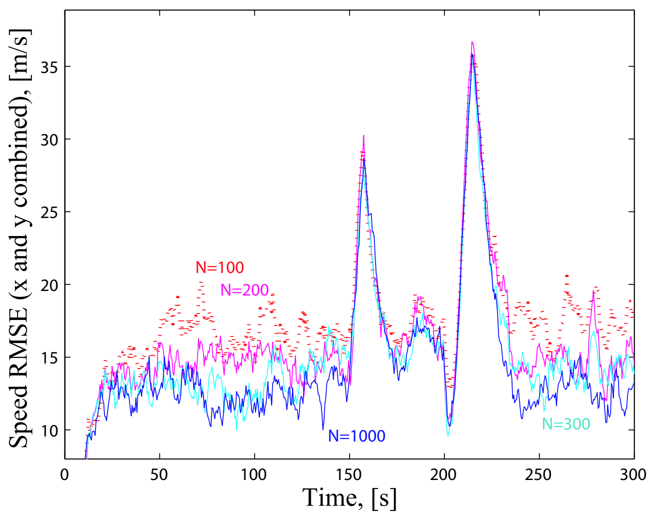

Fig. 9. Speed RMSE ($\dot{x}$ and $\dot{y}$ combined) of the RBPF with $N = 100,\ 200, 300, 500$ and 1000.

	RBPF					PF					EKF
N	100	200	300	500	1000	100	200	300	500	1000	
RMSE pos, [m]	228.5	204.1	193.5	193.2	192.4	303.8	223.2	199.7	184.2	177.0	303.5
RMSE speed, [m/s]	18.2	16.8	15.8	15.7	15.27	17.64	15.5	14.72	14.02	13.75	20.0
Time, [s]	0.097	0.191	0.301	0.517	1.07	0.097	0.185	0.284	0.467	0.9994	0.0011

Fig. 10. Table containing RMSEs (averaged over the whole time period) of the MC algorithms for different numbers of particles, from the EKF, and the respective computational time. All results are from 100 MC runs.

The robustness of the algorithms to outliers and missing data can be increased when the measurement error is modeled with a mixture of Gaussians [32]. In this particular implementation, we present results with one Gaussian component, $p(\boldsymbol{v}_k) = \mathcal{N}(\boldsymbol{\mu}_v, \boldsymbol{\sigma}_v^2)$, where the nonzero mean $\boldsymbol{\mu}_v$ and the covariance $\boldsymbol{\sigma}_v^2$ are calculated from RSSI data ($\boldsymbol{\mu}_v = (-1.96, -4.66, -3.23)'$, $\boldsymbol{\sigma}_v = \mathrm{diag}\{3.93, 6.99, 6.20\}$). The other parameters of the filters are: $\sigma_w = 0.00015$, $\alpha = 0.1$, $\eta = 4$, $V_{\max} = 10\ [m/s]$ and $\mathbb{M} = M_x \times M_y = \{(0.0, 0.0), (5.5, 0.0),\ (0.0, 5.5),\ (0.0, -5.5),\ (-5.5, 0.0)\}$.

The advantages of the MC methods compared to the EKF include their ability to easily incorporate constraints (e.g., speed, road constraints) and to deal efficiently with high level nonlinearities.

The behaviour of the MC filters is similar in both examples. Based on the above results we draw the following conclusions: *i*) The PF is sensitive to changes in the motion of the mobile unit. This sensitivity of the PF leads to higher peak-dynamic errors during abrupt manoeuvres. In the presence of a sequence of abrupt manoeuvres a divergence of the PF is not excluded if it operates with a small number of particles. The probability of divergence could be reduced if a high number of particles is used which, however, increases the computational complexity. *ii*) The RBPF exhibits better accuracy during the periods with abrupt changes. The 'measurements' at time instant k for the Kalman filter in the RBPF represent the difference between the estimated and predicted locations of the particles at time instances $k-1$ and k, respectively. This is one of the reasons

Fig. 11. The area in Glasgow, United Kingdom, where the vehicle is moving. The nearest BSs, the start and destination positions are indicated on the map.

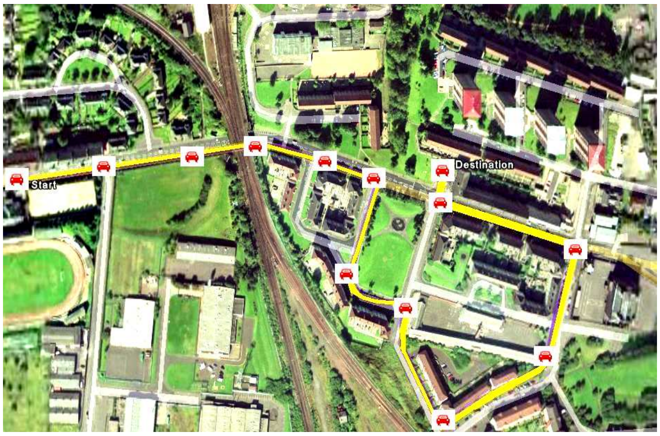

Fig. 12. The vehicle trajectory (from the left to the right side). The start and destination positions are indicated on the map.

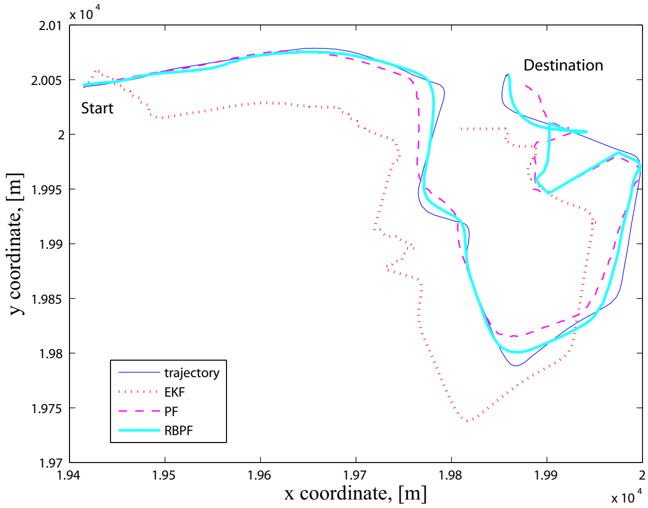

Fig. 13. Actual trajectory (from the GPS), and estimated trajectories by the EKF, PF and RBPF. $N = 1000$ particles are used in the MC algorithms.

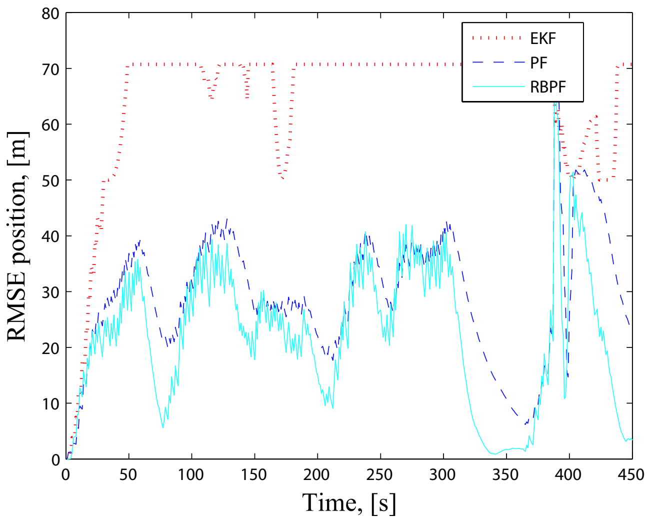

Fig. 14. Position RMSE of the EKF, PF and RBPF. $N = 1000$ particles are used in the MC algorithms.

for these particularities of its performance. Both MC filters outperform the EKF.

VIII. Conclusions

This paper has presented two sequential MC techniques for mobility tracking, namely a particle filter and a Rao-Blackwellised particle filter. An assessment of their best achievable theoretical accuracy has been made. They have shown efficient mobility tracking in wireless networks over both synthetic and real received signal strength measurements. The designed filters are compared with the EKF technique and their enhanced performance with respect to the EKF is demonstrated over scenarios with abrupt manoeuvres. Advantages of the RBPF compared with the PF are: *i*) decreased computational complexity because it exhibits similar accuracy with smaller number of particles; *ii*) smaller peak-dynamic errors during abrupt manoeuvres which is very important for the practice. Posterior Cramér-Rao lower bounds have been calculated that characterise the lower limit for the average mean-square error of the state estimates.

Open issues for future research include road-map assisted mobility tracking of single and multiple mobile units, investigation of different measurement models (including varying measurement time interval) and the fusion of data from different modalities.

IX. Acknowledgements

We would like also to thank the anonymous reviewers and Associate Editor for their constructive comments and suggestions. This research is sponsored by the Tracking Cluster project DIFDTC/CSIPC1/02 with the UK MOD Data and Information Fusion Defence Technology Centre, the EPSRC project EP/E027253/1 and partially by the Bulgarian Science Fund MI-1506/05 and Center of Excellence BIS21++, 016639.

References

[1] "Location is everything: positioning in wireless networks (a special issue)," *IEEE Signal Processing Mag.*, vol. 22, no. 4, July 2005.

[2] Z. R. Zaidi and B. L. Mark, "Real-time mobility tracking algorithms for cellular networks based on Kalman filtering," *IEEE Trans. Mobile Comput.*, vol. 4, no. 2, pp. 195–208, 2005.

[3] T. Liu, P. Bahl, and I. Chlamtac, "Mobility modeling, location tracking, and trajectory prediction in cellular networks," *IEEE J. Sel. Areas Commun.*, vol. 16, no. 6, pp. 922–936, Aug. 1998.

[4] B. Mark and Z. Zaidi, "Robust mobility tracking for cellular networks," in *Proc. IEEE Intl. Communications Conf.*, May 2002, pp. 445–449.

[5] H. Kobayashi, S.-Z. Yu, and B. Mark, "An integrated mobility and traffic model for resource allocation in wireless networks," in *Proc. 3rd ACM International Workshop on Wireless Mobile Multimedia*. ACM Press, 2000, pp. 39–47.

[6] S.-Z. Yu and H. Kobayashi, "A hidden semi-Markov model with missing data and multiple observation sequences for mobility tracking," *Signal Processing*, vol. 83, no. 2, pp. 235–250, 2003.

[7] Z. Yang and X. Wang, "Joint mobility tracking and hard handoff in cellular networks via sequential Monte Carlo filtering," in *Proc. IEEE Conf. on Computer Communications (Infocom) 2002*.

[8] Z. R. Zaidi and B. L. Mark, "Mobility estimation based on an autoregressive model," Electrical Engineering Department of George Mason University, USA, Tech. Rep., 2004.

[9] Y. Bar-Shalom and X. Li, *Estimation and Tracking: Principles, Techniques and Software*. Artech House, 1993.

[10] R. Moose, "An adaptive state estimator solution to the maneuvering target tracking problem," *IEEE Trans. Automatic Control*, vol. 20(3), pp. 359–362, June 1975.

[11] R. Singer, "Estimating optimal tracking filter performance for manned maneuvering targets," *IEEE Trans. Aerosp. Electron. Syst.*, vol. 6, pp. 473–483, July 1970.

[12] X. R. Li and V. Jilkov, "A survey of maneuveuvering target tracking, part I: Dynamic models," *IEEE Trans. Aerospace Electron. Syst.*, vol. 39, no. 4, pp. 1333–1364, 2003.

[13] L. Mihaylova, D. Bull, D. Angelova, and N. Canagarajah, "Mobility tracking in cellular networks with sequential Monte Carlo filters," in *Proc. Eight International Conf. on Information Fusion 2005*.

[14] M. Arulampalam, S. Maskell, N. Gordon, and T. Clapp, "A tutorial on particle filters for online nonlinear/non-Gaussian Bayesian tracking," *IEEE Trans. Signal Processing*, vol. 50, no. 2, pp. 174–188, 2002.

[15] J. Liu and R. Chen, "Sequential Monte Carlo methods for dynamic systems," *J. American Statistical Association*, vol. 93, no. 443, pp. 1032–1044, 1998.

[16] E. Wan and R. van der Merwe, *The Unscented Kalman Filter, Ch. 7: Kalman Filtering and Neural Networks, edited by S. Haykin*. Wiley Publishing, September 2001, pp. 221–280.

[17] B. Ristic, S. Arulampalam, and N. Gordon, *Beyond the Kalman Filter: Particle Filters for Tracking Applications*. Artech House, 2004.

[18] G. Casella and C. Robert, "Rao-Blackwellisation of sampling schemes," *Biometrica*, vol. 83, no. 1, pp. 84–94, 1996.

[19] P.-J. Nordlund and F. Gustafsson, "Sequential Monte Carlo filtering techniques applied to integrated navigation systems," in *Proc. American Control Conf.*, 2001, pp. 4375–4380.

[20] F. Gustafsson, F. Gunnarsson, N. Bergman, U. Forssell, J. Jansson, R. Karlsson, and P.-J. Nordlund, "Particle filters for positioning, navigation and tracking," *IEEE Trans. Signal Processing*, vol. 50, no. 2, pp. 425–437, 2002.

[21] P.-J. Nordlund, *Sequential Monte Carlo Filters and Integrated Navigation*. Licentiate Thesis, Linköping University, Sweden, 2002.

[22] T. Schön, F. Gustafsson, and P. Nordlund, "Marginalized particle filters for mixed linear/ nonlinear state-space models," *IEEE Trans. Signal Processing*, vol. 53, no. 7, pp. 2279–2289, July 2005.

[23] S. Maskell, M. Rollason, N. Gordon, and D. Salmond, "Efficient particle filtering for multiple target tracking with application to tracking in structural images," *Image and Video Computing*, vol. 21, no. 10, pp. 931–939, 2003.

[24] R. Chen and J. Liu, "Mixture Kalman filters," *J. Royal Stat. Soc. B*, vol. 62, pp. 493–508, 2000.

[25] A. Doucet, S. Godsill, and C. Andrieu, "On sequential Monte Carlo sampling methods for Bayesian filtering," *Statistics and Computing*, vol. 10, no. 3, pp. 197–208, 2000.

[26] C. Andrieu and A. Doucet, "Particle filtering for partially observed Gaussian state-space models," *J. of R. Statist. Soc. B.*, vol. 64, no. 4, pp. 827–836, 2002.

[27] N. Bergman, A. Doucet, and N. Gordon, "Optimal estimation and Cramér-Rao bounds for partial non-Gaussian state space models," *Ann. Inst. Statist. Math.*, vol. 53, no. 1, pp. 97–112, 2001.

[28] B. Ristic and M. Arulampalam, "Tracking a manoeuvring target using angle-only measurements: Algorithms and performance," *Signal Processing*, vol. 83, no. 6, pp. 1223–1238, 2003.

[29] P. Tichavsky, C. Muravchik, and A. Nehorai, "Posterior Cramér-Rao bounds for discrete-time nonlinear filtering," *IEEE Trans. Signal Processing*, vol. 46, no. 5, pp. 1386–1396, 1998.

[30] Y. Bar-Shalom, X. R. Li, and T. Kirubarajan, *Estimation with Applications to Tracking and Navigation*. John Wiley and Sons, 2001.

[31] R. Karlsson, T. Shön, and F. Gustafsson, "Complexity analysis of the marginalized particle filter," *IEEE Trans. Signal Processing*, vol. 53, no. 11, pp. 4408–4411, Nov. 2005.

[32] F. Gustafsson and F. Gunnarsson, "Mobile positioning using wireless networks: Possibilities and fundamental limitations based on available wireless network measurements," *IEEE Signal Processing Mag.*, vol. 22, no. 4, pp. 41–53, 2005.

Lyudmila Mihaylova is a Lecturer at the Department of Communication Systems, Lancaster University, United Kingdom. Prior this she was a Research Fellow with the Signal and Image Processing group at the University of Bristol, UK (2004-2006) and had visiting positions with the SYSTEMS group, at the University of Ghent, Belgium (2002-2004) and with the Robotics group of Katholieke Universiteit Leuven, Belgium (2000-2002). From 1996 to 2000 she was a Research Assistant at the Bulgarian Academy of Science and an Adjunct Assistant Professor at the Technical University of Sofia, Bulgaria. She received M.Sc. degree in Systems and Control Engineering (1989), M.Sc. degree in Applied Mathematics and Informatics (1991) and her Ph.D. degree in Systems and Control Engineering (1996), all from the Technical University of Sofia, Bulgaria. Her interests are in the area of nonlinear filtering, statistical signal and image processing, autonomous intelligent systems, and sensor data fusion. Dr. Mihaylova is a member of the IEEE, Signal Processing Society and of the International Society of Information Fusion.

Donka Angelova received the MS degree in mechanical engineering from the Technical University of Sofia, Bulgaria, a Ph.D. degree in Electrical Engineering. Currently, she is an Associate Research Professor of the Bulgarian Academy of Sciences (Institute for Parallel Information Processing) in Sofia, Bulgaria. She works as a key researcher and is involved in academic and industrial projects (Bulgarian and international) in the areas of multi-target tracking, detection and multi-sensor data fusion. The current research interests of Dr. Angelova includes the application of sequential Monte Carlo methods to the problems of applied nonlinear estimation and filtering and decision making

Souroush Honary has background in Satellite Communications and GNSS Positioning systems and he was an engineer firstly at DERA Defford, and then at Visteon Corporation (where he was involved within the design of Navigation Systems and Electronic Toll Collection for the German 'Toll Collect' project). Since leaving Visteon Corporation to move to HW Communications Ltd in 2002, Souroush has applied extensive research into methods for overcoming vulnerabilities within GNSS based solutions. More recently, his research has been more focused upon ubiquitous positioning by utilising surrounding communication infrastructures. Dr Honary currently has the lead role for the integration and validation of advanced hybrid positioning within EU framework 6 project DAIDALOS, where significant advancements to A-GPS and GSM/802.11 positioning are in progress. His key responsibilities within this EU Framework 6 project include: Development of context aware location determination techniques MANET Multi-Hop positioning which will enable Mobile Terminals to make use of the positioning capabilities of other Mobile Terminals in close proximity, and Work for multi-layered hybrid mobile positioning protocols.

David Bull is Professor of Signal Processing and Head of the Electrical and Electronic Engineering Department at the University of Bristol, United Kingdom. Prior to his current appointment he has been a Systems Engineer at Rolls Royce and subsequently a Lecturer at Cardiff University. He leads the Signal Processing activities within the Centre for Communications Research where he is Deputy Director. He has been a member of the UK Foresight Panel and the Steering Group for the DTI/EPSRC LINK programme in Broadcast Technology and is currently on the EPSRC Peer Review College. He is a past director of the VCE in Digital Broadcasting and Multimedia Technology and is currently Chairman and Technical Director of ProVision Communication Technologies Ltd., specialising in wireless multimedia communications. David Bull has worked widely in the fields of 1 and 2-D signal processing and has published over 250 papers, various articles and two books. He has won two IEE Premium awards for this work. His current research is focused on the problems of image and video communications for both low bit rate wireless, internet and broadcast applications. In particular he is working on error resilient source coding, linear and non-linear filterbanks, scalable coding methods, motion estimation, data fusion and architectural optimisation.

Nishan Canagarajah is Professor of Multimedia Signal Processing at Bristol, United Kingdom. Prior to this he was an Research Assistant and lecturer at Bristol investigating digital signal processing (DSP) aspects of mobile radio receivers. He has BA (Hons) and a Ph.D. in DSP Techniques for Speech Enhancement both from the University of Cambridge. His research interests include image and video coding, image segmentation, content based video retrieval, 3D video, image fusion and the application of signal processing to audio and medical electronics. He is widely supported in these areas by industry, EU and the EPSRC. He has been involved in a number of FP5 and FP6 projects where the team has been developing novel image/video processing algorithms. He has published more than 150 papers and two books. He is a member of the EPSRC College.

Branko Ristic received a B.Eng. degree from the University of Novi Sad (Serbia) in 1984, and his M.Sc. degree from Belgrade University (Serbia) in 1991, both in Electrical Engineering. He received a PhD in Signal Processing from Queensland University of Technology (Australia) in 1995. Between 1984 and 1994 he held various reserach/engineering positions at IBK Institute Vinca (Belgrade), Queensland University, and QUT in Brisbane. During 1995 he was a Senior DSP engineer in GEC Marconi Systems (Sydney) and since 1996 he is a senior research scientist with DSTO, Australia. During 2003/04 he spent a year in IRIDIA (Université libre de Bruxelles, Belgium) on a study leave. His main research interests include target tracking, sensor fusion, belief function theory, non-linear filtering. He published over 80 technical papers and co-authored the book *Beyond the Kalman filter*, Artech House, 2004. He co-developed and currently lectures a post-graduate course “Multi-Sensor Data Fusion” at the University of Adelaide. He served on technical committees of several international conferences and received twice the best paper award at international conferences.